Null Geodesics from Ladder Molecules

Anish Bhattacharya¹, Abhishek Mathur², and Sumati Surya³

¹Indian Institute of Science, Bangalore, 560012, India
²Chennai Mathematical Institute, Kelambakkam, Tamil Nadu, 603103, India
³Raman Research Institute, Sadashivanagar, Bangalore 560080, India

Abstract

We propose a discrete analogue of null geodesics in causal sets that are approximated by \mathbb{M}^2 , in the spirit of Kronheimer and Penrose's "grids" and "beams" for an abstract causal space. The causal set analogues are "ladder molecules", whose rungs are linked pairs of elements corresponding loosely to Barton et al's horizon bi-atoms [1]. In \mathbb{M}^2 a ladder molecule traps a ribbon of null geodesics corresponding to a thickened or fuzzed out horizon. The existence of a ladder between linked pairs of elements in turn provides a generalisation of the horismotic relation to causal sets. Simulations of causal sets approximated by a region of \mathbb{M}^2 show that ladder molecules are fairly dense in the causal set, and provide a light-cone like grid. Moreover, similar to the uniqueness of null geodesics between horismotically related events in \mathbb{M}^2 , in such causal sets there is a unique ladder molecule between any two linked pairs which are related by the generalised horismotic relation.

"To admit structures which can be very different from a manifold. The possibility arises, for example, of a locally countable or discrete event-space equipped with causal relations macroscopically similar to those of a space-time continuum."

- Kronheimer and Penrose on the aims of studying axiomatic causal spaces [2].

Kronheimer and Penrose's (KP) abstract causal spaces come equipped with the order relations, \leq (causal) and \ll (chronological) [2]¹. These are required to be acyclic (thus preventing closed causal and chronological curves), with each satisfying transitivity individually, and together, a mixed transitivity condition. The KP causal spaces are therefore posets with respect to both \leq and \ll separately, with \leq strictly larger than the relation \ll . A third, the horismotic relation \rightarrow , is obtained from the first two by the simple exclusion:

¹Here \leq is reflexive, i.e., $x \leq x$ and \prec is irreflexive, $x \prec\!\!\!/ x$.

 $x \leq y, x \not\prec y \Rightarrow x \rightarrow y$. It is used by KP to build "girders" and "beams" which provide the abstract analogs of the null-geodesics of a continuum spacetime.

Causal posets are also the fundamental building blocks in causal set theory [3, 4]. In this approach to quantum gravity, continuum spacetime is approximated by a locally finite poset or causal set, with the order relation \leq corresponding to the causal order of the spacetime. The requirement of local finiteness allows a correspondence between the number of elements in a causal interval n and the continuum spacetime volume V. In the continuum approximation which we denote by $C \sim (M, g)$ this is realised on average as $\langle n \rangle = \rho V$, where ρ^{-1} is the spacetime discreteness scale. The average is obtained from a random Poisson sprinkling of points into (M, g) at density ρ , with probability $P_V(n) = \frac{(\rho V)^n}{n!} e^{-\rho V}$. For each realisation, a causal set is assembled from the sprinkled points using the induced causal ordering from (M, g).

The Poisson sprinkling process is uniform with respect to the spacetime volume which means that null related elements are a set of measure zero. Thus the elements in $C \sim (M, g)$ are almost surely only related via the chronological relationship \prec in (M, g). Because the chronological relation is irreflexive, it is therefore more appropriate to use the irreflexive \prec symbol for causal sets. The closest analogue of a null-like relation between elements in a causal set is a link or nearest neighbour relation \prec * where $e \prec *e' \Rightarrow \not \supseteq e''$, $e \prec e'' \prec e'$. For a causal set C which is approximated by d-dimensional Minkowski spacetime \mathbb{M}^d , for example, the elements linked to any $e \in C$ "hug" the future and past light cone of e. However, these links are almost surely time-like. While they can be used to roughly characterise the light-cones, they cannot substitute for a null-relation; a link in $C \sim \mathbb{M}^d$ that hugs the light-cone in one frame can be far from null in another frame. Thus one cannot make a Lorentz invariant statement about the "null-ness" of a single link. In order to obtain a truly null-relation, one would therefore need the right combination of time-like and space-like related elements.

Null hypersurfaces are of course important in several contexts, not least as black hole horizons. In causal set theory there has been considerable success in extracting geometric information from the causal order, including discrete versions of proper time, spatial topology, scalar field propagators and the Einstein-Hilbert action, which help in establishing a robust correlation between the continuum approximation and the underlying causal set ensemble. However, an intrinsic definition of null hypersurfaces is still lacking. In [1] "horizon molecules", which are a class of sub-causal sets, were defined using the help of a continuum spatial hypersurface Σ and a null hypersurface \mathcal{N} . Σ and \mathcal{N} divide the spacetime into four regions $M_-^- \equiv J^-(\Sigma) \cap J^-(\mathcal{N})$, $M_+^+ \equiv J^-(\Sigma) \cap J^+(\mathcal{N})$, $M_+^+ \equiv J^+(\Sigma) \cap J^-(\mathcal{N})$ and $M_+^+ \equiv J^+(\Sigma) \cap J^+(\mathcal{N})$. Labelling the corresponding causal set regions $C_-^-, C_+^-, C_+^+, C_+^+, C_+^+$, respectively, the horizon n-molecule is a subcauset $\{p,q^{(1)},...,q^{(n)}\}$ such that (i) $p \prec q^{(k)} \cup \{p\}$ are the only elements in both C_+^- and in the future of p. It was shown that in the limit of large sprinkling density ρ , the number of horizon molecules is proportional to the area of the intersection $\mathcal{A} = \Sigma \cap \mathcal{N}$.

While this construction is very powerful and works for any pair (Σ, \mathcal{N}) , the question remains – what intrinsically is a horizon in a causal set? Inspired by the KP construction of null geodesics as "beams" as well as the horizon molecule construction we take a first step in this direction. Ours is a proposal for constructing null geodesics in $C \sim \mathbb{M}^2$; since each null geodesic in \mathbb{M}^2 is also a null hypersurface trivially, it is also therefore a proposal for a causal set horizon. Conversely, it allows us to define a discrete horismotic relation. We now describe this proposal and show results from simulations that lend support to it. Our discussion is strictly for d = 2; the analogous construction in \mathbb{M}^d for d > 2 does not result from a straightforward generalisation of the d = 2 case. At the end of this paper we discuss a possible generalisation to higher d.

We begin with the definition of the simplest horizon molecule or bi-atom H_2 associated with (\mathcal{N}, Σ) . This is a linked pair (p,q) in $C \sim (M,g)$ where (a) $p \in I^-(\mathcal{N}) \cap I^-(\Sigma)$,(b) $q \in I^+(\mathcal{N}) \cap I^-(\Sigma)$, (c) q is the only point in $I^+(p) \cap I^-(\Sigma)$. This implies that q is maximal in $C|_{I^+(\mathcal{N})\cap I^-(\Sigma)}$ and p is maximal in $C|_{I^-(\mathcal{N})\cap I^-(\Sigma)}$. Because of the fundamental discreteness of causal sets H_2 is also a horizon molecule for an entire continuum family of $\{(\mathcal{N}, \Sigma)\}$. Fig 1 depicts the associated "thickened" horizon and spatial hypersurface for a single H_2 . This suggests that any discrete analogue of a horizon will correspond at best to a thickened horizon in the continuum.

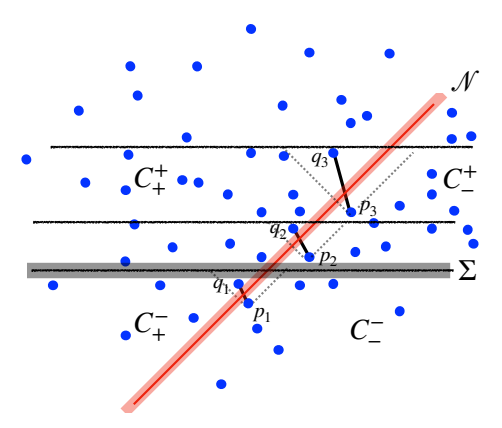


Figure 1: The horizon bi-atoms H_2^i associated with a family of spatial hypersurfaces which intersect a null hypersurface \mathcal{N} . These are "stacked" one on top of the other but do not form a ladder molecule. \mathcal{N} and the bottom-most spatial hypersurface Σ are also "thickened" to depict a family of (\mathcal{N}, Σ) which share the same horizon bi-atom H_2^1 made up of the linked pair $\{p_1, q_1\}$. The regions $C_{\pm}^{\pm} \subset C$ depicted are with respect to Σ .

In order to motivate our construction we consider a discrete family of Σ_i and the associated horizon molecules H_2^i for each $\mathcal{N} \cap \Sigma_i$ as shown in Fig 1. Given such a "stack" of H_2^i , we can think of them as guides for a thickened horizon. However since the H_2^i are not intrinsically defined, this is not sufficient for our purpose. Instead we consider stacks of linked pairs $h_i = (p_i, q_i), p_i \prec *q_i$. In order to recover a null geodesic, we must stack these one on top of the other in a suitable and intrinsic manner so that, when embed-

ded in the continuum they trap a ribbon of null geodesics. We denote the causal interval by $[p,q] \equiv \{r \in C | r \in \text{Future}(p) \cap \text{Past}(q)\}$, where $\text{Future}(p) \equiv \{r \in C | p \prec r\}$ and $\text{Past}(p) \equiv \{r \in C | r \prec p\}$. Importantly, because of the use of the irreflexive relation \prec , $p,q \notin [p,q]$

We construct a ladder molecule L_k step by step as follows. Let $L_1 \equiv h_1$ where $h_1 = (p_1, q_1), p_1 \prec *q_1$ be the first rung. The next rung $h_2 = (p_2, q_2), p_2 \prec *q_2$ must satisfy the stacking condition

$$p_1 \prec p_2, q_1 \prec q_2, p_1 \prec q_2, |[p_1, q_2]| = 2.$$
 (1)

The rung h_2 is thus "stacked" on top of the rung h_1 in a causally rigid manner since no elements other than those in h_1, h_2 are allowed in the interval $[p_1, q_2]$. L_2 is then the 4-element diamond sub-causal set, with the pair q_1, p_2 space-like to each other. More generally, we build L_k from L_{k-1} by stacking $h_k = (p_k, q_k)$ on top of L_{k-1} such that

$$p_{k-1} \prec * p_k, q_{k-1} \prec * q_k, |[p_{k-i}, q_k]| = 2i, |[p_i, p_j]| = j - i - 1, |[q_i, q_j]| = j - i - 1.$$
 (2)

Thus, $|[p_1, q_k]| = 2(k-1)$, with the pairs p_i, q_j being space-like to each other for all j < i. This volume rigidity that goes all the way down the ladder ensures that it is "as straight as possible". It is important to note here that although inspired by the horizon molecules, typically stacks of horizon bi-atoms do not form ladders as depicted in Fig 1.

As shown in Fig 2 the L_k trap a ribbon of null geodesics in \mathbb{M}^2 , which we define as follows. Let \mathcal{P} denote the set of all inextendible null geodesics in \mathbb{M}^2 . The ribbon of null geodesics associated with an L_k is

$$\mathcal{N}_k(L_k) \equiv \{ \eta \in \mathcal{P} | \eta \cap J^+(q_1) = \emptyset, \eta \cap J^-(p_k) = \emptyset \}.$$
 (3)

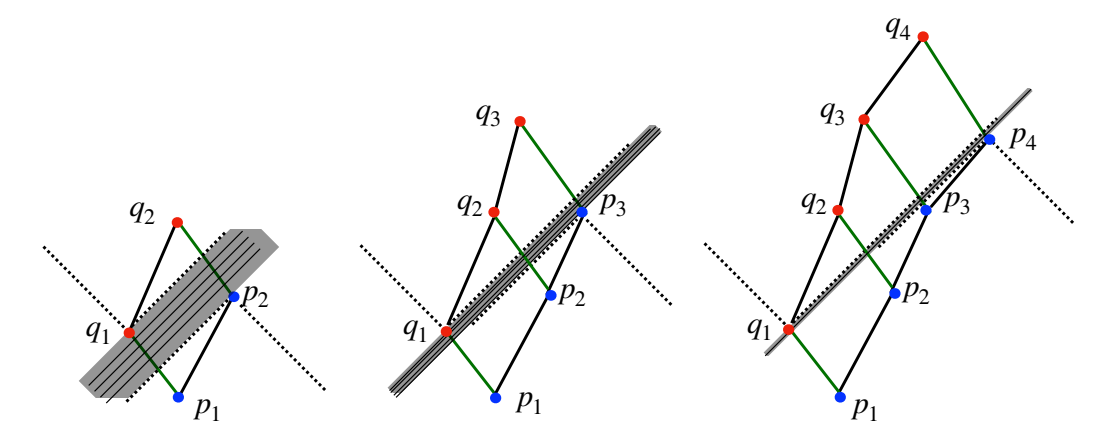


Figure 2: Illustrations of ladder molecules L_2, L_3, L_4 and the associated ribbons of null geodesics. As more rungs are added the ribbons become narrower.

We now use the ladder molecules to generalise the horismotic relation to causal sets. We say that the linked pairs $h = (p, q), p \prec *q$ and $h' = (p', q'), p' \prec *q'$ are discrete horismotically

related

$$h \to h' \text{ if } \exists L_k, k \ge 2, L_k|_1 = h, L_k|_k = h'.$$
 (4)

where $L_k|_i = h_i$ denotes the *i*th rung of an L_k . As in the case of the horismotic relation, \rightarrow does not satisfy transitivity:

$$h \rightarrow h', h' \rightarrow h'' \not\Rightarrow h \rightarrow h'',$$
 (5)

since the two ladders L from h to h' and L' from h' to h" while sharing a rung h' (and thus being causally ordered) may not satisfy the various rigidity conditions between elements in L and those in L'. This is similar to the horismotic relation in the continuum where $a \to b$, $b \to c \not\Rightarrow a \to c$. We know that unlike the chronological relation, if $p \to q$ then there exists a unique future directed null geodesic from p to q in \mathbb{M}^2 . Is this also true for the relation \to ? As we discuss below there is numerical evidence to suggest that this is indeed the case.

In \mathbb{M}^2 we can go further since we need only two independent null directions ∂_u, ∂_v to define a tangent basis. As we have defined them, the ladders do not carry an intrinsic direction that would help assign a family of right movers or left movers to them without the embedding. Consider the causal diamond L_2 with rungs $h_1, h_2, h_1 \rightarrow h_2$. Since the pair q_1, p_2 are space-like, with both linked to p_1 to the past and q_2 to their future it can also be viewed as the ladder L'_2 with $h'_1 = (p_1, p_2), h'_2 = (q_1, q_2)$, where $q_1 \leftrightarrow p_2$. Thus, one can "grow" a ladder L_k, L'_k either using the h_2 rung or the h'_2 rung as shown in Fig 3. These two ladders then correspond to the two null directions ∂_u, ∂_v "at" L_2 . We will call this double ladder a V_k sub-causal set.

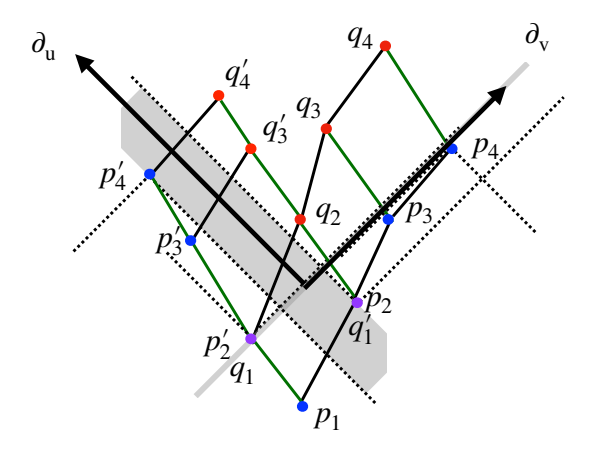


Figure 3: An illustration of a V_4 sub-causal set and the directions ∂_u , ∂_v that can be obtained from it.

Since we were motivated by the horizon bi-atoms, we can now ask whether the rungs of the ladder molecules are in fact horizon molecules of a given spatial hypersurface. In the continuum this is trivially the case since we can always "fit" in a Σ . In the discrete setting the analogue of a spatial hypersurface is an antichain. If we take the antichain A_i

associated with $h_i = (p_i, q_i)$ as one that "threads" through q_i , but is to the past of p_{i+1} , then the intersection of the discrete horizon with \mathcal{A}_i is just q_i . The "area" of this intersection is then proportional to the number of horizon molecules as in [1].

The first question we must address is whether ladders occur often enough in $C \sim \mathbb{M}^2$ to make this definition a useful one in our characterisation of null geodesics in C. Starting with a linked pair $h_1 = (p_1, q_1)$, how likely it is that there is a next rung $h_2 = (p_2, q_2)$, and a next one and so on? Since a ladder L_k embeds² in \mathbb{M}^2 for any k > 1, an L_k with $L_k|_1 = h_1$ almost surely exists in \mathbb{M}^2 since there is infinite room, so to speak, to find the next rung and the next³. What is more relevant however is the density of ladders in a given bounded region of \mathbb{M}^2 . In [6] the abundance of k-element intervals in a causal diamond in \mathbb{M}^d was calculated analytically as a function of sprinkling density and the volume of the causal diamond. While the ladders are 2(k-1) element intervals, they are not the only causal sets in this class. For example, for k=2, there are two causal sets which are 2-element intervals: the causal diamond poset L_2 and the 4-element totally ordered set or chain. The calculations of [6] do not tell us anything about the more detailed distributions of specific sub-causal sets.

Since we have defined the L_k using the the discrete intervals the likelihood can be assessed by looking at the associated continuum volumes in a Poisson sprinkling. For every $x \in \mathbb{M}^2$ there are invariant hyperbolae defined by the volume V of the Alexandrov interval between any point on this hyperbola and x (or equivalently, its proper time $\sqrt{2V}$ to x) both to the future and the past. Let $v_k(x)$ denote the region between the future invariant hyperbolae of discrete volume $k - \sqrt{k}$ and $k + \sqrt{k}$ about x where $k = \rho V$, and we have included the Poisson fluctuations of order $\sqrt{\rho V}$.

Let us start with the likelihood of finding an L_2 associated with a given p_1 . For $p_1 \prec *q_1$ the interval $[p_1, q_1]$ should be empty, and hence q_1 is most likely to lie in the region $v_1(p_1)$ between the future light cone of p_1 , i.e., at $k = 1 - \sqrt{1} = 0$ and the invariant hyperbola at discrete spacetime volume at $k = 1 + \sqrt{1} = 2$. This is a region of infinite spacetime volume and hence almost surely there exists a pair $h_1 = \{p_1, q_1\}$. Next, we look for p_2 where $p_1 \prec *p_2$. Since the volume of $v_1(p_1)$ is infinite, such a p_2 can again almost surely be found. The conditions on q_2 are however much more stringent since not only should $p_2 \prec *q_2$ and $q_1 \prec *q_2$, but also $|[p_1, q_2]| = 2$, i.e., $q_2 \in v_1(q_1) \cap v_1(p_2) \cap v_3(p_1)$. For such a q_2 to be sufficiently likely, the discrete volume $\rho \text{vol}(v_1(q_1) \cap v_1(p_2) \cap v_3(p_1)) \gtrsim 1$.

First we look at the region $CEDFC \equiv v_1(q_1) \cap v_1(p_2)$ which is itself finite as shown in Fig 4, when the proper space-like distance $d = d(q_1, p_2) > 0$. We can always choose coordinates such that $q_1 = (0, -d/2)$ and $p_2 = (0, d/2)$. In this case, $C = (d/2, 0), D = (\sqrt{d^2/4 + 4}, 0), E = (2/d + d/2, 2/d), F = (2/d + d/2, -2/d)$. CEDFC is symmetric about x = 0 and bounded by the curves $t^2 - (x + d/2)^2 = 4$ (upper boundary of $v_1(q_1)$), $v_2 - (x - d/2)$

²An embedding $C \hookrightarrow M$ does not require the number-volume correspondence to hold. Not all causal sets embed in \mathbb{M}^2 . However, the fact that the ladder does embed *does not* mean that it is in any sense typical.

³Spaces of infinite extent allow all kinds of possibilities for causal sets, but may not be physically relevant. For example, while a void the size of the present universe almost surely occurs in \mathbb{M}^d , the probability for a Fermi-radius sized void within the Hubble radius is essentially zero, as shown in [5].

 $(d/2)^2 = 4$ (upper boundary of $(v_2(p_2))$) and the null ray t = x + d/2 from (q_1) and the null ray (t = x - d/2) from (p_2) . Thus, its volume is

$$V(d) = 2\left(\int_0^{2/d} \left(\sqrt{\left(x - \frac{d}{2}\right)^2 + 4} - (x + d/2)dx\right)\right)$$
$$= 4\sinh^{-1}\left(\frac{4 - d^2}{4d}\right) + 4\sinh^{-1}\left(\frac{d}{4}\right) - 2 + \frac{d}{4}\left(\sqrt{d^2 + 16} - d\right)$$
(6)

which monotonically decreases with d, becoming infinite as $d \to 0$. For $d < d_0 \sim 2.23$ the discrete volume $\gtrsim 1$.

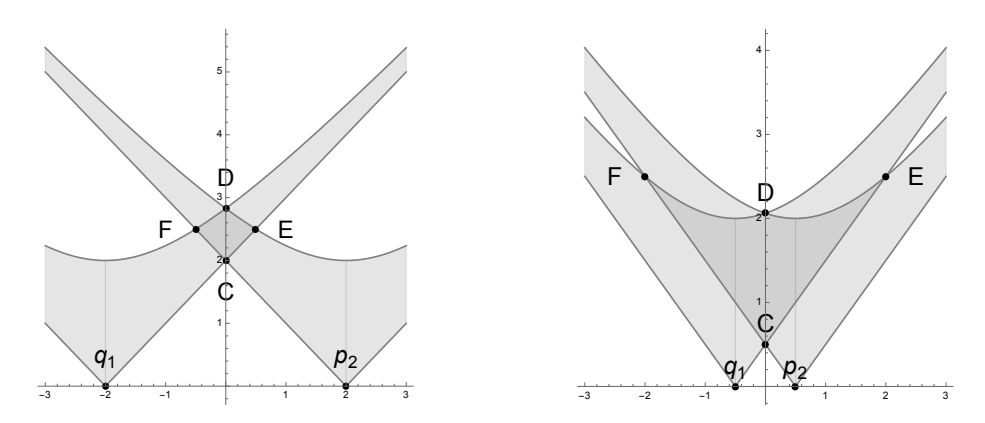
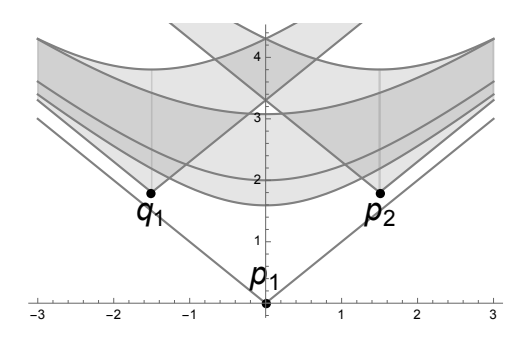


Figure 4: As the proper distance between q_1 and p_2 decreases, the overlap region CEDFC (shaded dark gray) increases monotonically.

The tricky part of course is to ensure that the further overlap with $v_3(p_1)$ is large enough. Fig 5 illustrates the fact that when d is too large the overlap is zero, while the overlap can be significant for smaller d. In order to calculate the volume of the overlap region, we make a simplifying assumption that q_1 and p_2 are symmetrically to the future of p_1 , i.e., if $p_1=(0,0)$ then we assume $q_1=(T,-d/2), p_2=(T,d/2)$ (which is of course not strictly possible in the causal set.) The overlap region $CEDFC=v_1(q_1)\cap v_1(p_2)$ has $C=(d/2+T,0), D=(\sqrt{d^2/4+4}+T,0)$ and E=(d/2+2/d+T,2/d) and F=(d/2+2/d+T,-2/d) while the boundary hyperbolae of $v_3(p_1)$ intersect the t-axis at $\tau_-=(\sqrt{6-2\sqrt{3}},0)$ and $\tau_+=(\sqrt{6+2\sqrt{3}},0)$. Here there are two parameters d and d, but because the lower boundary of $v_3(p_1)$ is at d and d and d and d are the overlap with d and d are the case for d and d and d are the overlap is finite, and the question is whether there is a "sweet spot" in d for which this overlap is large but also probable.

Calculating this analytically is messy, since there are a large number of possible types of intersections of CEDFC with $v_3(p_1)$ leading to different formulae for the volume. We



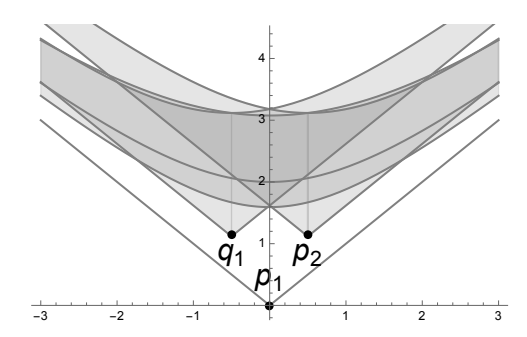


Figure 5: The overlap region $O \equiv v_1(q_1) \cap v_1(p_2) \cap v_3(p_1)$ for two different choices of d and T. q_1, p_2 lie in the tregion $v_1(p_1)$ which is unshaded, but overlaps with the shaded region $v_3(p_1)$. In the figure on the left d and T are large enough that O is empty: the CEDFC region lies entirely above $v_3(p_1)$. In the figure on the right d and T values are small enough to make the overlap (the darkest shaded region) O non-empty.

instead turn to numerical simulations to help us determine the abundance of the L_2 in a causal diamond. Fig 6 gives an idea of the growth of the L_2 as a function of n. Comparing with the analytic expression of [6] we see that the diamonds are roughly the same in number as the remaining 2-element intervals, namely the 4-element chain. Note that the 4-element chains are intrinsically more "time-like", and hence can stray further away from null directions. The causal diamond interval on the other hand has both time-like $(p_1 \text{ and } q_2)$ and space-like $(q_1 \text{ and } p_2)$ relations, which force it into a more null-like configuration.

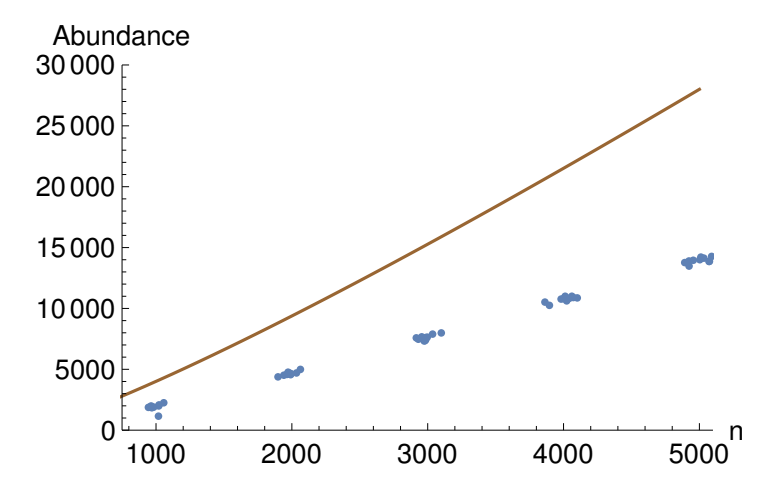


Figure 6: The abundance of causal diamond intervals in a causal diamond in \mathbb{M}^2 as a function of n. We compare it with the analytic expression for the abundance of all 2-element intervals depicted by a solid line.

In the rest of the paper we present results on numerical simulations of causal sets. We

find that the L_k for k=2,3,4 are not rare even in finite regions of \mathbb{M}^2 . We calibrate the density of these discrete null geodesics by using the embedding in \mathbb{M}^2 to obtain the null ribbons and find that they form a dense null grid on the causal set. We also find that that for small k values the V_k causal sets while not common, do exist, thus providing local ∂_u , ∂_v directions in the causal set. Finally we find that the ladders satisfy a uniqueness condition, "upto q_k ". This suggests a discrete version of Penrose's Proposition 2.19 [7] (see below) for the generalised horismotic relation \rightarrow .

For numerical convenience in what follows we consider sprinklings into a half diamond in \mathbb{M}^2 rather than the full diamond, for

$$n \sim 500, 1000, 2000, 3000, 5000, 7000, 10000, 12000, 15000, 18000.$$
 (7)

and perform 10 trials for each value of n. We search for the L_k starting with a p_1 in the bottom n/10 of the elements as shown in Fig 7. We restrict our search to k = 2, 3, 4, since already for k = 4, the abundance is very small.

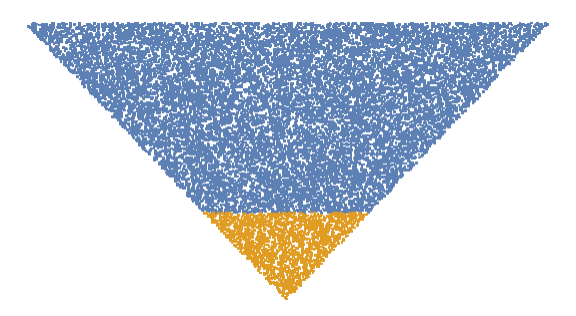


Figure 7: The p_1 are chosen from the bottom $\sim n/10$ th set of sprinkled elements.

Fig 8 shows the number of ladders for k = 2, 3, 4 as a function of n on a log-log plot. There is a clear scaling behaviour of the abundance of L_k , i.e., $N(L_k) \sim a_k n^{\alpha_k}$, with a_k a decreasing function of k with the exponent α_k being approximately k independent. Thus the abundance decreases with k as expected, with a significant population of k = 2, 3 ladders compared to k = 4.

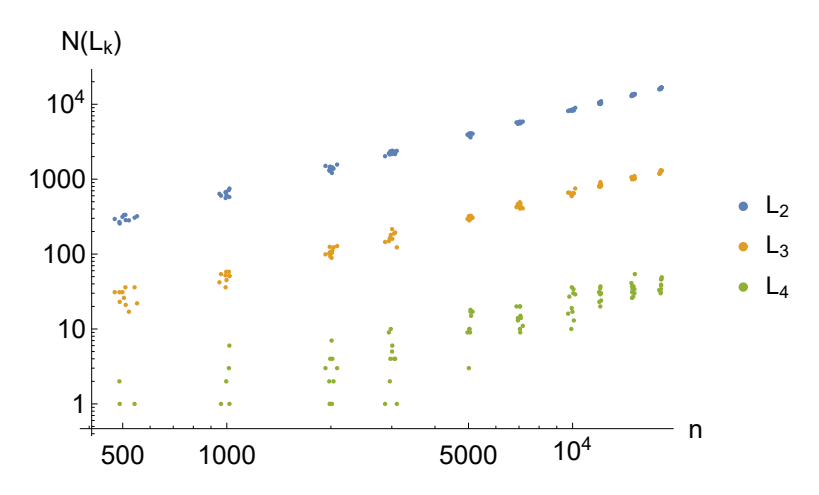


Figure 8: A log-log plot of the abundance of L_k with n.

The L_k are moreover statistically significant enough to form a dense "grid" of null geodesics in \mathbb{M}^2 . In Fig 9 we plot the null ribbons associated with every L_3 and L_4 which has been generated in a particular sprinkling with $n \sim 18,000$. These form a dense null grid in \mathbb{M}^2 , the former more dense than the latter.

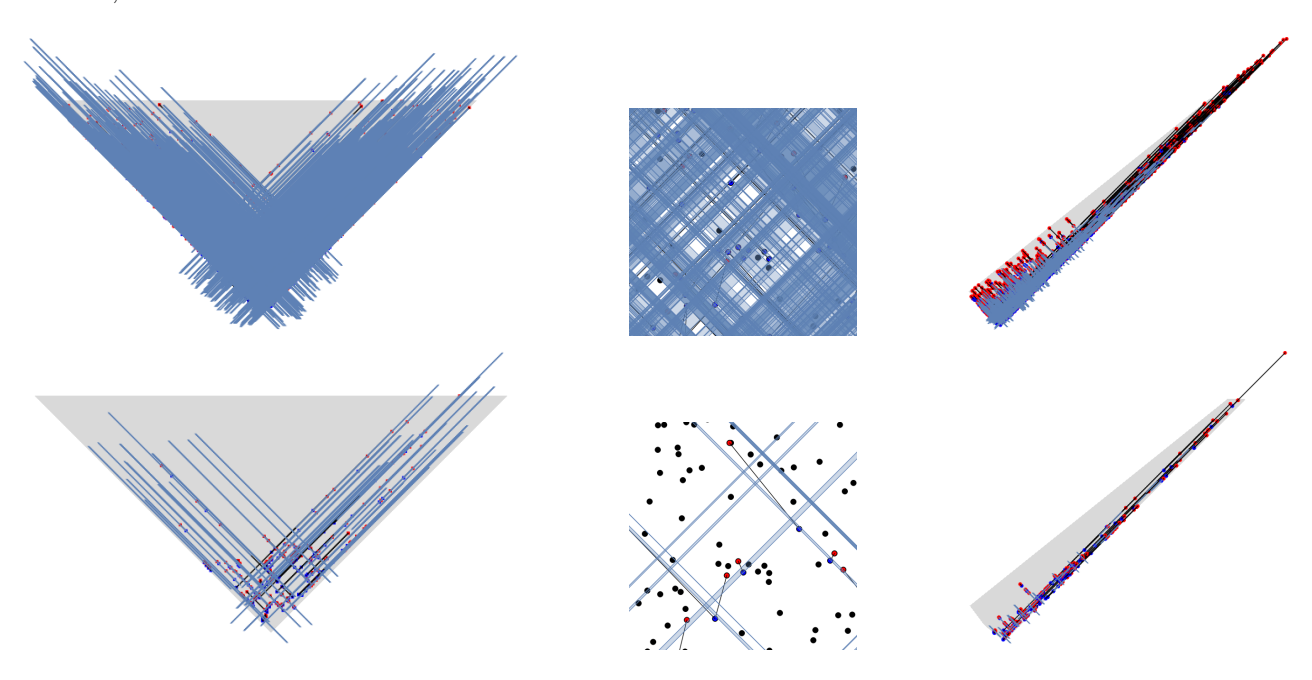


Figure 9: The null grid formed by L_3 and L_4 ladders in an $n \sim 18,000$ sprinkling. We show the same zoomed-in region in both cases, as well as the entire Lorentz transformed region. The grid for L_3 is far more dense than for L_4 and is fine enough to reach the discreteness scale.

In Fig 10 we show a specific example of an L_4 ladder and the associated null ribbon

for different boost parameters, for an $n \sim 18,000$ sprinkling. As expected, the null ribbon "fattens" or "thins" depending on the choice of β . In \mathbb{M}^2 there is a simple Lorentz invariant quantity associated with the ribbon. This is the causal volume associated with the unique pair (x,y), $x \to q_1, x \to p_n$ and $q_1 \to y, p_n \to y$. The volume of [x,y] is therefore an invariant under a Lorentz transformation. Thus, one can squeeze or fatten the ribbon without changing this volume.

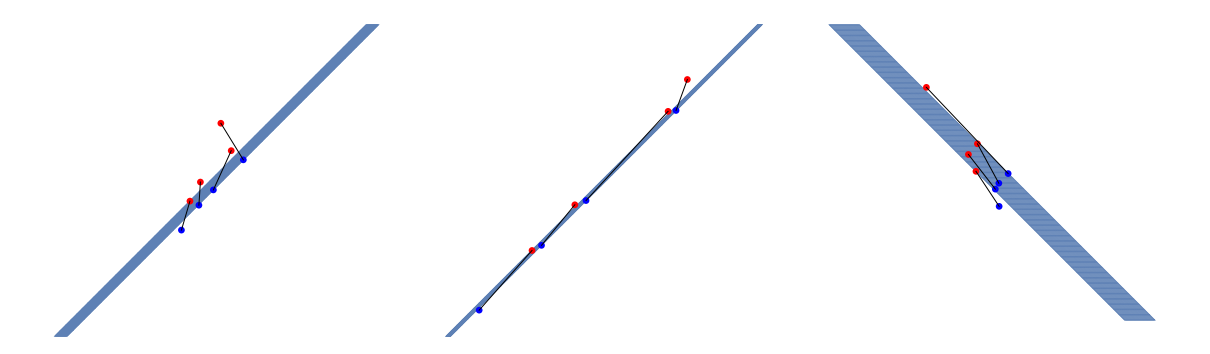


Figure 10: An L_4 ladder in an $n \sim 18,000$ sprinkling with boost parameters (a) $\beta = 0$ (b) $\beta = 0.8$ (c) $\beta = -0.8$. The p_i are depicted in blue while the q_i are depicted in red.

Our simulations also give rise to intersecting or V-type ribbons of the type shown in Fig 3. These are however far fewer than the ladders. For V_3 , we show the number of occurence in Fig 11. In Fig 12 we show the only example of a V_4 that resulted from our simulations.

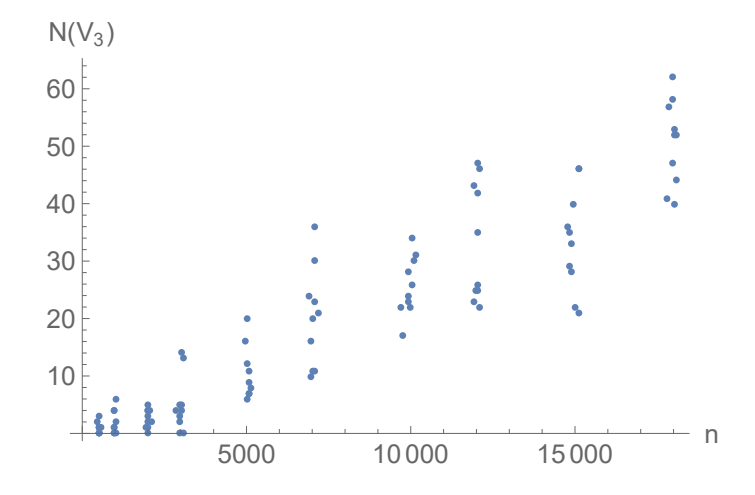


Figure 11: The abundance of V_3 as a function of n.

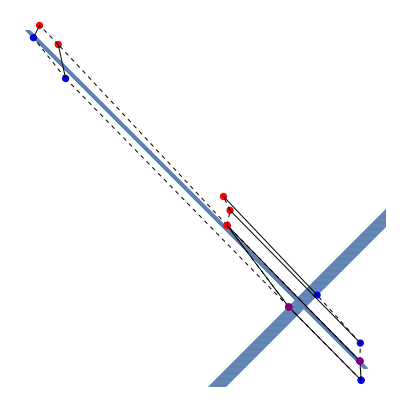


Figure 12: An example of an V_4 subcausal set, using which we obtain an intrinsic characterisation of the directions $\partial_{\mathbf{u}}$, $\partial_{\mathbf{v}}$. The purple points are the pairs $(q_1, p_2) = (p'_2, q'_1)$. As before, the p_i, p'_i are depicted in blue and the q_i, q'_i in red.

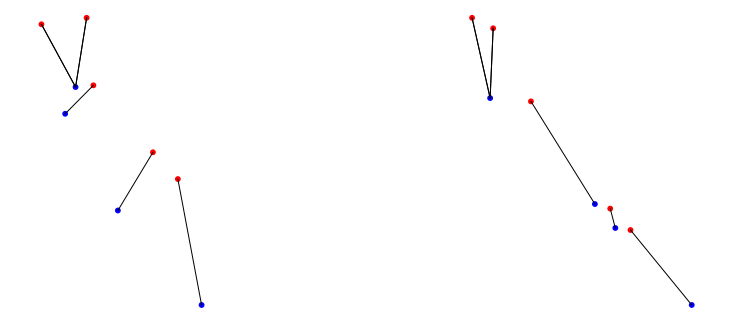


Figure 13: Two examples of L_4 , which are unique "upto" q_4 . Given h_1 and h_4 , there is a unique L_4 from h_1 to h_4 . However h_4 itself is not unique and so we have a second ladder L'_4 from h_1 to h'_4 . Such non-uniqueness however gets ironed out as one goes to higher k, as is the case with the L_3 's.

Proposition 2.19 of Penrose's monograph [7] states that:

Proposition:. (Penrose) If α is a null geodesic from a to b and β is a null geodesic from b to c, then either $a \prec\!\!\!\!\!/ b$ or else $\alpha \cup \beta$ constitutes a single null geodesic from a to c.

Our simulations lend support to the following generalisation thus providing the strongest evidence that ladders are indeed the analogues of null geodesics in causal sets that embed into \mathbb{M}^2 :

Conjecture:. If L_k , k > 1 is a ladder from h to h' and $L'_{k'}$, k' > 1 is a ladder from h' to h'', where the h, h', h'' are linked pairs of elements, then either $h \not\rightarrow h''$ or else $L_k \cup L'_{k'}$ constitutes a single ladder $L_{k+k'-1}$ from h to h''.

We have taken the first steps towards a geometric reconstruction of null geodesics in manifold like causal sets. The construction presented above is limited to \mathbb{M}^2 but because all spacetimes in d=2 are conformally related it is likely that this construction will go through for curved d=2 spacetimes. The generalisation to higher dimensions is non-trivial and currently being investigated. Any definition of null-ladders should be able to trap an entire d-dimensional pencil of null-geodesics for it to be realised in the causal set via a Poisson process. Hence the d=2 null ribbon construction cannot suffice in higher dimensions. A proposal currently being investigated is to use (d-1) horizon molecules as the rungs of the null ladder with $p \prec q^{(i)}$, $i=1,\ldots d-1$ forming a (d-1) "simplex" whose (d-1) face has a space-like normal. Constructing the ladder molecule requires the $q^{(i)}$ from different rungs to be tied together suitably in order to make the ladder as straight as possible. Numerical investigations of such a ladder molecule construction in d=3 are underway.

Our work is numerical, more out of simplicity than necessity. Integrals for calculating the probabilities of ladder molecules are easily defined but non-trivial to calculate analytically, since several simultaneous conditions must be met by each ladder element. While the interval abundance calculations of [6] give complex, but closed form expressions, preliminary work on ladder molecules suggests otherwise. Numerical investigations of this causal set architecture will therefore remain a robust tool in investigating generalised ladder molecules in higher dimensions.

Acknowledgements: We thank the organisers of the conference SCRI21 (where one of the authors was a speaker) for their invitation to submit a contribution to this collection. This work as well as many aspects of the causal set approach to quantum gravity are strongly influenced by Roger Penrose's ideas on causal structure.

The datasets generated during and/or analysed during the current study are available from the corresponding author on reasonable request.

References

- [1] C. Barton, A. Counsell, F. Dowker, D. S. W. Gould, I. Jubb, and G. Taylor, "Horizon molecules in causal set theory," *Phys. Rev. D*, vol. 100, no. 12, p. 126008, 2019.
- [2] E. H. Kronheimer and R. Penrose, "On the Structure of causal spaces," *Proc. Cambridge Phil. Soc.*, vol. 63, pp. 481–501, 1967.
- [3] L. Bombelli, J. Lee, D. Meyer, and R. Sorkin, "Space-Time as a Causal Set," *Phys. Rev. Lett.*, vol. 59, pp. 521–524, 1987.

- [4] S. Surya, "The causal set approach to quantum gravity," *Living Rev. Rel.*, vol. 22, no. 1, p. 5, 2019.
- [5] F. Dowker, J. Henson, and R. D. Sorkin, "Quantum gravity phenomenology, Lorentz invariance and discreteness," *Mod. Phys. Lett. A*, vol. 19, pp. 1829–1840, 2004.
- [6] L. Glaser and S. Surya, "Towards a Definition of Locality in a Manifoldlike Causal Set," *Phys. Rev. D*, vol. 88, no. 12, p. 124026, 2013.
- [7] R. Penrose, *Techniques of Differential Topology in Relativity*. Society for Industrial and Applied Mathematics, 1972.